




Pre-clinical evaluation of biomarkers for the early detection of nephrotoxicity following alpha-particle radioligand therapy

Mengshi Li¹ · Claudia Robles-Planells² · Dijie Liu¹ · Stephen A. Graves³ · Gabriela Vasquez-Martinez² · Gabriel Mayoral-Andrade² · Dongyoul Lee⁴ · Prerna Rastogi⁵ · Brenna M. Marks¹ · Edwin A. Sagastume¹ · Robert M. Weiss⁶ · Sarah C. Linn-Peirano^{2,7} · Frances L. Johnson¹ · Michael K. Schultz^{1,3,8} · Diana Zepeda-Orozco^{2,9,10} 

Received: 7 May 2023 / Accepted: 1 December 2023 / Published online: 14 December 2023
© The Author(s) 2023

Abstract

Purpose Cancer treatment with alpha-emitter-based radioligand therapies (α -RLTs) demonstrates promising tumor responses. Radiolabeled peptides are filtered through glomeruli, followed by potential reabsorption of a fraction by proximal tubules, which may cause acute kidney injury (AKI) and chronic kidney disease (CKD). Because tubular cells are considered the primary site of radiopeptides' renal reabsorption and potential injury, the current use of kidney biomarkers of glomerular functional loss limits the evaluation of possible nephrotoxicity and its early detection. This study aimed to investigate whether urinary secretion of tubular injury biomarkers could be used as an additional non-invasive sensitive diagnostic tool to identify unrecognizable tubular damage and risk of long-term α -RLT nephrotoxicity.

Methods A bifunctional cyclic peptide, melanocortin 1 ligand (MC1L), labeled with [²⁰³Pb]Pb-MC1L, was used for [²¹²Pb]Pb-MC1L biodistribution and absorbed dose measurements in CD-1 Elite mice. Mice were treated with [²¹²Pb]Pb-MC1L in a dose-escalation study up to levels of radioactivity intended to induce kidney injury. The approach enabled prospective kidney functional and injury biomarker evaluation and late kidney histological analysis to validate these biomarkers.

Results Biodistribution analysis identified [²¹²Pb]Pb-MC1L reabsorption in kidneys with a dose deposition of 2.8, 8.9, and 20 Gy for 0.9, 3.0, and 6.7 MBq injected [²¹²Pb]Pb-MC1L doses, respectively. As expected, mice receiving 6.7 MBq had significant weight loss and CKD evidence based on serum creatinine, cystatin C, and kidney histological alterations 28 weeks after treatment. A dose-dependent urinary neutrophil gelatinase-associated lipocalin (NGAL, tubular injury biomarker) urinary excretion the day after [²¹²Pb]Pb-MC1L treatment highly correlated with the severity of late tubulointerstitial injury and histological findings.

Conclusion Urine NGAL secretion could be a potential early diagnostic tool to identify unrecognized tubular damage and predict long-term α -RLT-related nephrotoxicity.

Keywords Radiopeptide ligand therapies · Alpha-emitter · Dosimetry · Nephrotoxicity · Biomarkers · NGAL

Introduction

Radioligand therapies (RLTs) have emerged as a form of therapy in oncology that has the potential to be transformative for cancer patients. These radiopharmaceuticals consist of a radionuclide coupled to a small peptide ligand that binds to cell membrane targets with high affinity and specificity, making these agents attractive as cancer therapeutics

(Fig. 1a). Unlike external beam radiation therapy (EBRT), these targeted forms of systemic radiotherapy enable radionuclides to be delivered directly to cancer cells. Examples of FDA-approved radiopharmaceuticals that are significantly improving outcomes for cancer patients include beta (β)-particle-emitting RLT LUTATHERA® (i.e., [¹⁷⁷Lu]Lu-DOTATATE) for advanced neuroendocrine tumors (NETs) and PLUVICTO® (i.e., [¹⁷⁷Lu]Lu-PSMA-617) for metastatic castrate-resistant prostate cancer (mCRPC) targeting somatostatin receptor type 2 (SSTR2) and prostate-specific membrane antigen (PSMA), respectively. RLTs are also effective in other SSTR-expressing tumors, such as

Mengshi Li and Claudia Robles-Planells are co-first authors.

Extended author information available on the last page of the article

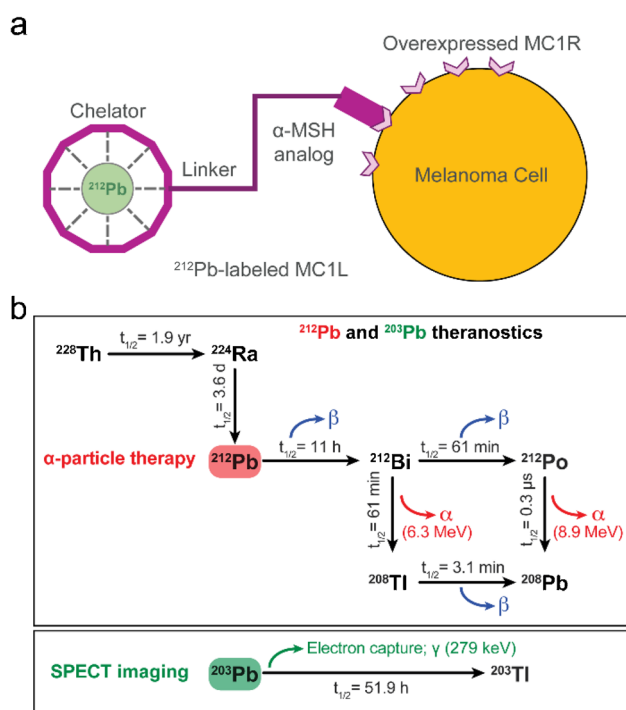


Fig. 1 **a** Schematic representation of [^{212}Pb]Pb-labeled melanocortin 1 ligand (MC1L), melanoma cell expressing melanocortin 1 receptor (MC1R), and alpha-melanocyte-stimulating hormone (α -MSH) analog. **b** Schematic representation of [^{212}Pb] and [^{203}Pb] nuclides decay

paraganglioma and pheochromocytoma, thyroid carcinoma, and meningioma [1]. The use of other ligands for overexpressed receptor targets has been demonstrated in breast, colon, myeloma, and ovarian cancer [1]; melanoma [2]; and hematological malignancies [3]. There is a significant difference in the observed efficacy of RLTs that is dependent on the radionuclide utilized. Compared to FDA-approved β -emitter drugs, recent studies using alpha (α)-emitter RLTs (e.g., ^{212}Pb , ^{225}Ac , ^{211}At) in patients with NET and mCRPC demonstrate greater tumor cell cytotoxicity, including patients with refractory disease following β -RLT [4]. Fundamentally, the advantages of α -emitters lie in the higher linear-energy transfer (LET) ($\sim 100 \text{ keV}/\mu\text{m}$), which induces double-strand DNA breaks (DSB) and a concomitant increase in ionizations (primary and secondary) along their short path length in the cellular tissue microenvironment [5]. The deposition of energy over extremely short path length results in a significantly increased incidence of lethal DSB, high relative biological effectiveness (RBE), improved tumor-cell-cytotoxicity, and activation of anti-tumor immunity [6]. Among commercially available α -emitters, [^{212}Pb] (half-life $T_{1/2}$ 10.6 h) is produced using a [^{224}Ra]/[^{212}Pb] generator system that enables nimble on-demand production of [^{212}Pb]Pb-based radiopharmaceuticals [7]. In the case of [^{212}Pb], the isotope [^{203}Pb] ($T_{1/2}$ 51.9 h) can be used as a

single-photon emission computerized tomography (SPECT) imaging diagnostic companion to provide detailed dosimetry that guides [^{212}Pb] therapy dosing [8]. The [^{203}Pb]/[^{212}Pb] radionuclide pair has the advantage that elementally identical imaging surrogate [^{203}Pb] can guide [^{212}Pb] therapy (Fig. 1b). Here, we establish biomarkers that can be used in the pre-clinical setting to connect surrogate imaging information to the potential for acute kidney injury (AKI) to more effectively use the imaging data to establish appropriate therapeutic dosing strategies. It is envisioned that these data can lead not only to more effective dose planning for clinical translation of new RLTs but for a broader spectrum of pharmaceutical drug candidates for clinical introduction for cancer therapy.

While emerging research demonstrates the potentially transformative impact of α -particle RLT for cancer treatment, kidneys are often treatment-limiting due to their role in the bioelimination of unbound therapeutic agents. While agents can be pharmacologically designed to minimize the reabsorption, biomarkers that provide information on the potential for nephrotoxicity are needed because current evaluation is limited to late post-therapy histological findings and estimation of glomerular filtration rate (eGFR) using the endogenous marker of kidney function serum creatinine (sCr). Fortunately, due to their relatively small size ($< 5.5 \text{ kDa}$) and hydrophilic nature, radiolabeled peptides are rapidly filtered through glomeruli. However, a fraction can be reabsorbed in tubular cells, which may lead to injury [9]. Studies in tubule-specific megalin knockout mice demonstrate that proximal tubules are primarily, but not exclusively, responsible for radiopeptide uptake within the kidneys [10]. Because of the short travel distance of emitted particles (low-energy $\beta < 1.7 \text{ mm}^1$; $\alpha < 80 \mu\text{m}$), the radiation exposure from RLT, especially α -RLT, may be highly localized in the proximal tubular area rather than glomeruli. This suggestion is further supported by prior pre-clinical studies evaluating nephrotoxicity of alpha- and beta-emitter RLT that demonstrated the presence of tubulointerstitial disease as early as 10 weeks, without significant glomerular changes, which progressively worsens and leads to severe chronic kidney disease (CKD) 7 months after therapy [11, 12]. This observation is consistent with the known pathophysiology of AKI-induced CKD, wherein primary tubular cells that fail to repair after severe or recurrent injuries adopt a pro-fibrotic and pro-inflammatory phenotype that drives progressive kidney damage resulting in structural abnormalities including fibrosis, vascular rarefaction, tubular loss, glomerulosclerosis, and a chronic inflammatory infiltrate, with subsequent renal function decline [13]. Thus, primary

¹ Low-energy beta emitters ([^{177}Lu], [^{67}Cu], [^{131}I]), does not include higher energy emitters ([^{90}Y], [^{89}Sr], [^{32}P], etc.).

tubular damage alone could be the etiology of RLT-induced long-term kidney toxicity.

Current nephrotoxicity screening for assessing pharmaceutical-treated patients and mice for establishing potential kidney injury depends mainly on prospective sCr measurement and its routine use to calculate eGFR. Kidney toxicity in patients receiving RLT is expected to be associated with patchy loss of tubule cells, focal areas of proximal tubular dilation, and distal tubular casts, together with measurements of cellular regeneration [14]. Serum creatinine is a delayed and insensitive biomarker of kidney function decline that does not reflect the degree of tubulointerstitial damage. Additionally, long-term toxicity evaluation is limited by the patient population's poor survival. In comparison, urinary biomarkers such as neutrophil gelatinase-associated lipocalin (NGAL), kidney injury molecule 1 (KIM-1), and epidermal growth factor (EGF) have been used to detect AKI early in patients with normal sCr (subclinical AKI) and to evaluate overall tubular health [15]. The change in their urinary secretion pattern has been used to identify patients at risk of progressive CKD [16]. Predictive biomarkers could accurately identify patients with subclinical kidney injury and those at risk of AKI and CKD following RLT treatment.

Regulatory bodies currently employ 23 Gy in kidneys as the absorbed dose limit, derived from EBRT, despite significant differences in the form and interaction of radioactivity emissions associated with RLT vs. EBRT. For example, the typical dose rate for EBRT is ~1 Gy/min, whereas the absorbed dose from RLT is delivered over multiple days, even weeks, depending on the half-life of the radionuclide, resulting in a slower dose rate (mGy/min). Although conventional EBRT dose limits may differ from those encountered with RLT, dosimetry-based therapy remains a potentially powerful tool for personalizing RLT. Specifically, in RLT, a biologically effective dose of 40 Gy to the kidney has been suggested to be safe in patients without risk factors for kidney disease and 28 Gy in those at risk of kidney injury [17]. A more precise understanding of the nature of kidney-delivered doses may help maximize cancer therapy and reduce long-term kidney toxicity according to individual patient tolerability. However, this approach is limited by the need for more information on tubular damage caused by a specific kidney-absorbed dose not provided by sCr measurement. Thus, the purpose of this study was to investigate the urinary secretion pattern of tubular injury biomarkers following injection of a [²¹²Pb]Pb-based RLT in a murine model. In this dose-escalation study, a bifunctional cyclic peptide, melanocortin 1 ligand (MC1L), was labeled with [²⁰³Pb]Pb-MC1L to determine the distribution and absorbed dose of [²¹²Pb]Pb-MC1L at levels intended to

induce AKI, followed by a comprehensive nephrotoxicity analysis including novel urine secretion pattern of kidney injury biomarkers in CD-1 Elite mice. To explore potential absorbed dose tolerated in humans, we performed human dosimetry scaling up from mice. It is envisioned that combining biomarkers and dosimetry can lead to a more detailed understanding of the use of [²⁰³Pb]-based imaging as a quantitative guide for [²¹²Pb] therapy planning and a personalized approach to cancer therapy.

Methods

Reagents and materials

Detailed information on reagents and material used in this study can be found in the Supplemental Methods section.

Radiochemistry, in vivo biodistribution of [²⁰³Pb]Pb-MC1L, and dosimetry of [²¹²Pb]Pb-MC1L

Radiochemistry radiolabeling and quality control of [²⁰³Pb]/[²¹²Pb]Pb-MC1L were performed as previously described [6] and are detailed in the Supplemental Methods section. Biodistribution of [²⁰³Pb]Pb-MC1L in normal organs/tissues was determined in male CD-1 Elite mice. All animal studies followed the Guide for the Care and Use of Laboratory Animals and were approved by the University of Iowa Animal Care and Use Committee. Mice were injected with 74 MBq [²⁰³Pb]Pb-MC1L (2–100 pmol injected peptide) in 100 µL saline via tail vein and were subsequently euthanized at 0.5, 1.5, 3, and 24 h post-injection for organs/tissues resection ($n = 4–6$ at each time point). Radioactivity in each organ was measured on a Cobra II automated gamma counter and decay corrected. Data were normalized and expressed as percent injected dose per gram of tissue (%ID/g). The absorbed dose from [²¹²Pb]Pb-MC1L injection in mouse and human was calculated using the [²⁰³Pb]Pb-MC1L surrogate biodistribution data using typical medical internal radiation dose (MIRD) absorbed fraction methods within the OLINDA/EXM v2.2 software. Detailed dosimetry calculations are described in the Supplemental Methods section.

Treatment to evaluate alpha-emitter toxicity

Male CD-1 Elite mice were treated with a dose-escalation regiment to evaluate toxicity at levels intended to cause kidney injury. Mice were administered either 0.0 (vehicle), 0.9, 3.0, or 6.7 MBq [²¹²Pb]Pb-MC1L (injected peptide mass 0.0–0.6 nmole, $n = 6$ per group) as single injection via tail vein on day 0. No lysine co-injection was conducted to ensure kidney damage induction by [²¹²Pb]Pb-MC1L.

Following treatments, the body weight of individual animals was measured twice weekly during the acute stage (i.e., the first 3 weeks post-injection) and once per week in later stages.

Hematotoxicity, blood chemistry, and cardiotoxicity

Hematotoxicity, liver toxicity, and cardiac structure and function were assessed as described in the Supplemental Methods section.

Urine nephrotoxicity biomarkers

Biomarkers of kidney injury and tubular health were measured in urine samples collected using metabolic cages at 1 week (days 1 and 3), 8 weeks, and 28 weeks (7 months) post-[²¹²Pb]Pb-MC1L injection. Murine metabolic cages from Hatteras Instruments (Grantsboro, NC) were kindly provided by Dr. Jonathan Nizar at the Department of Internal Medicine at The University of Iowa. After collection, urine samples were kept on ice and centrifuged at 2000 rpm for 5 min to remove particulates, and the supernatant was stored in a –80 °C freezer until the analysis day. Urine NGAL, KIM-1, EGF, and protein and creatinine levels were measured as detailed in the Supplemental Methods section.

Kidney histological analysis

Twenty-eight weeks post [²¹²Pb]Pb-MC1L injection, mice were euthanized. Kidneys were fixed in 4% paraformaldehyde and embedded in paraffin. Tissue Sects. (5 μm thick) were stained with periodic acid-Schiff (PAS) for tubular injury (TI), glomeruli changes (GC), and interstitial inflammation (IF) semiquantitative evaluation. To measure renal interstitial fibrosis, paraffin-embedded kidney sections were stained with Masson's trichrome. A blinded pathologist performed scoring as described in Supplemental Table 1.

Statistical and correlation analysis

Statistical analysis was conducted on GraphPad Prism 8 (GraphPad Software, San Diego, CA, USA). Two-way ANOVA was applied in CBC, serum chemistry, and serum biomarkers **p* < 0.05. The Kruskal–Wallis test was applied for histological score analysis, with * *p* < 0.05. Urine biomarkers and body weight statistical analysis was made by two-way ANOVA mixed-effect analysis with **p* < 0.05. Correlation analysis was made by computed nonparametric Spearman correlation for urine biomarkers and multiparameter correlation.

Results

Biodistribution of [²⁰³Pb]Pb-MC1L and dosimetry of [²¹²Pb]Pb-MC1L

To determine [²¹²Pb]Pb-MC1L absorbed dose in critical organs (e.g., kidneys), we employed [²⁰³Pb]Pb-MC1L as a dosimetry surrogate in the in vivo biodistribution study in male CD-1 Elite mice. Following i.v. injection of 74 kBq [²⁰³Pb]Pb-MC1L, there was a rapid [²⁰³Pb]Pb-MC1L clearance through the kidneys and bladder (8.2%; Fig. 2a). Within 1.5 h post-injection, the remaining [²⁰³Pb]Pb-MC1L in blood was 0.06%ID/g. The highest kidney accumulation (8.2%ID/g) was at 0.5 h post-injection, with minimal accumulation in other organs. As intended, [²⁰³Pb]Pb-MC1L retention in kidneys was relatively low (1.9%ID/g at 24 h) but higher than in other organs, resulting in higher radiation exposure, enabling our evaluation of biomarkers. We used this information to perform a dosimetry analysis within the MIRD schema to determine the absorbed dose in the kidneys resulting from administering [²¹²Pb]Pb-MC1L in male CD-1 mice. Based on the OLINDA/EXM 2.2 35-g mouse phantom, the average absorbed dose per injected activity in kidneys was 2.99 Gy/MBq, among which 92.7% resulted from α-radiation (Fig. 2b), with an estimated tubular and glomerular dose per administered activity of 4.85 Gy/MBq and 12.51 Gy/MBq, respectively (implementation of the Hobbs et al. model is detailed in the Supplemental Methods) [18]. Thus, the kidney-absorbed doses in male CD-1 mice delivered from 0.9, 3.0, and 6.7 MBq [²¹²Pb]Pb-MC1L were 2.8, 8.9, and 20 Gy on average. Detailed murine dosimetry results are summarized in Supplemental Tables 5 and 6. Finally, to determine a human absorbed dose from this therapy, we performed dosimetry in human subjects scaling up from mice as described in Supplemental Methods. Co-localizing progeny with parent [²¹²Pb], the predicted human absorbed radiation dose in kidneys was 5.34 mGy/MBq, among which 4.76 mGy/MBq is contributed by α-radiation. Due to the rapid clearance and minimal accumulation in bone, the predicted human absorbed dose in red marrow was 0.26 mGy/MBq. Murine and human dosimetry results are summarized in Fig. 3 and Supplemental Tables 6 and 7, respectively.

Systemic, cardiac, and liver toxicity

To identify [²¹²Pb]Pb-MC1L chronic toxicity complications, the study was completed at 28 weeks after treatment, as this represents one-third of the expected lifespan of these animals (Fig. 4a). No acute weight loss was observed

Fig. 2 **a** Biodistribution of $[^{203}\text{Pb}]\text{Pb-MC1L}$ in male CD-1 Elite mice. **b** Kidney dosimetry of $[^{212}\text{Pb}]\text{Pb-MC1L}$ in male CD-1 Elite mice

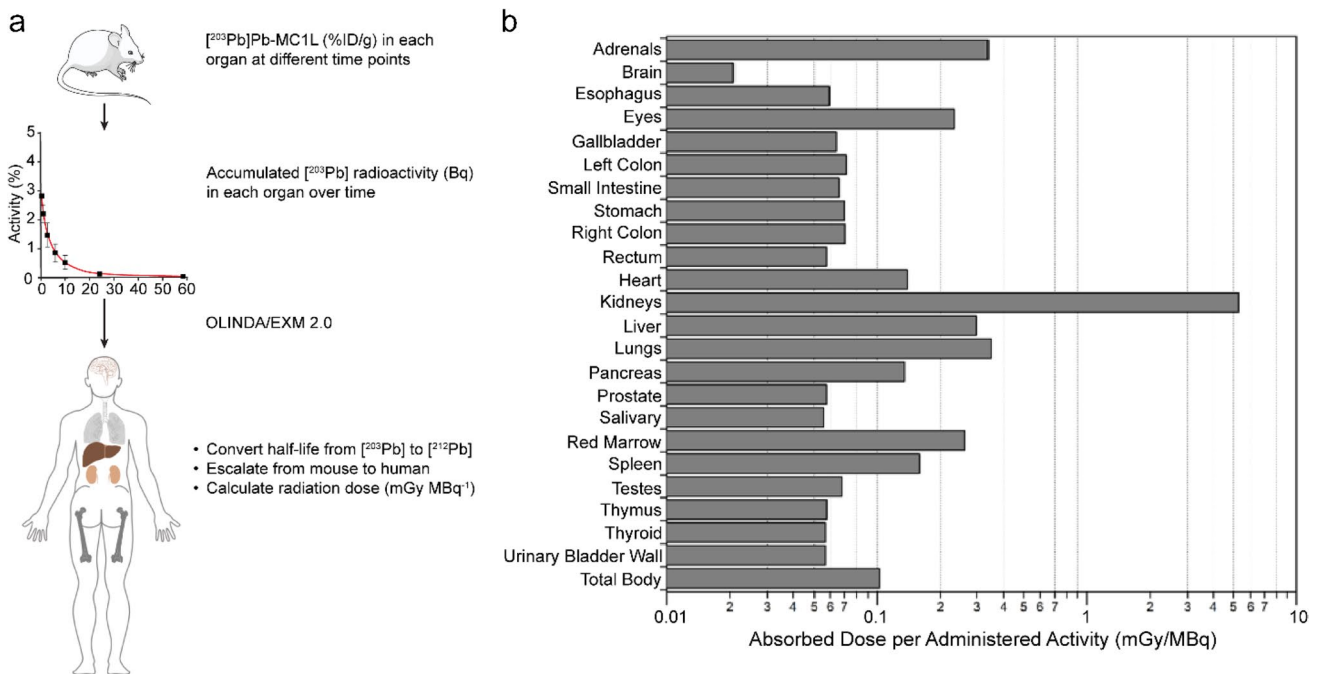
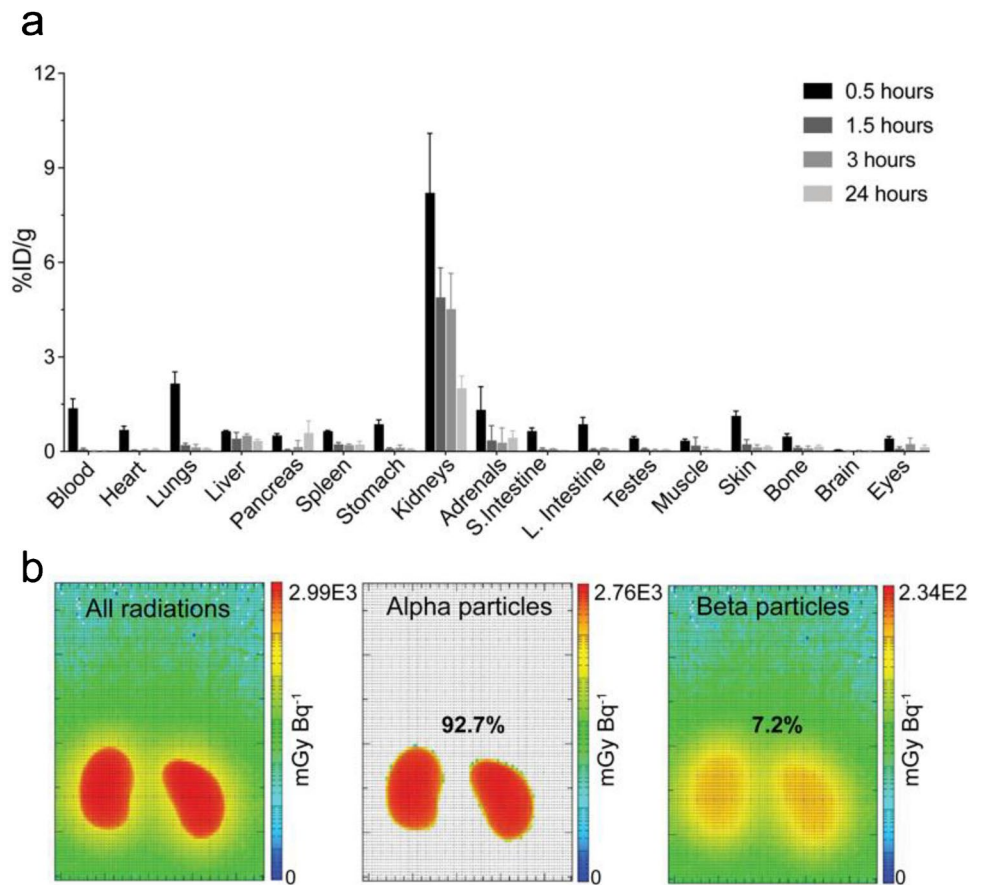


Fig. 3 **a** Representative figure of how radiation dose was estimated in humans. **b** Dosimetry analysis of $[^{212}\text{Pb}]\text{Pb-MC1L}$ in female and male human subject Phantoms in OLINDA/EXM 2.0

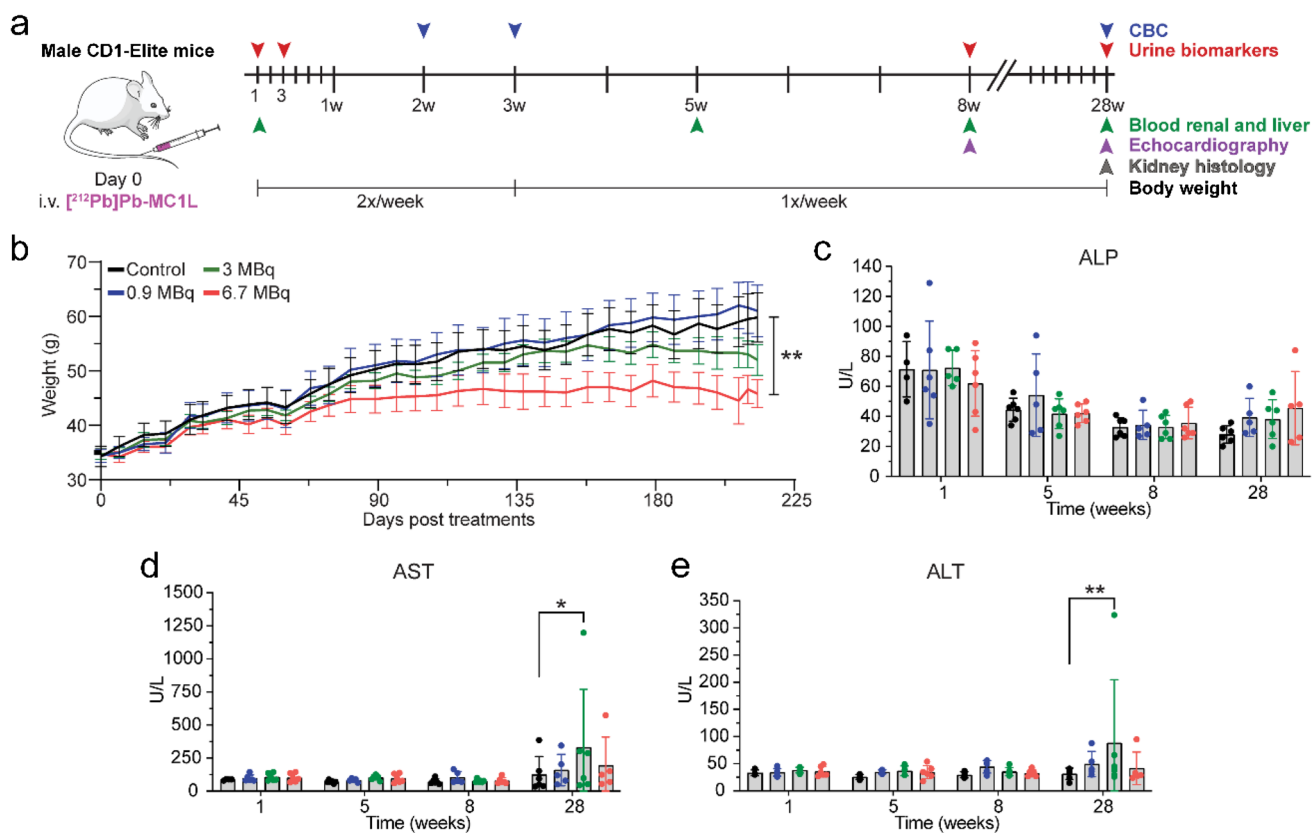


Fig. 4 **a** Experiment design. **b** Body weight in male CD-1 Elite. **c–e** Liver function measurement by serum chemistry analysis. Statistical analysis was made by two-way ANOVA analysis with $*p < 0.05$

in any $[^{212}\text{Pb}]\text{Pb-MC1L}$ -treated mice. However, mice treated with 6.7 MBq of $[^{212}\text{Pb}]\text{Pb-MC1L}$ demonstrated a lack of weight gain that initiated about 50 days post-treatment and was significantly different compared to the control group after 28 weeks (45.8 ± 5.8 g vs. 59.8 ± 11.2 g, $p = 0.0056$, Fig. 4b).

Cardiac structure and function were analyzed by echocardiogram at 8 and 28 weeks post-treatment. No significant cardiac structural or functional changes were identified with the evaluation of heart rate, left ventricular mass, end-diastolic volume, and ejection fraction in $[^{212}\text{Pb}]\text{Pb-MC1L}$ -treated mice (Supplemental Fig. 1).

There was no significant change in the liver injury markers ALT, AST, and ALP (Fig. 4c–e) in the first 8 weeks post-treatment. There was a higher concentration of AST and ALT in animals treated with 3.0 MBq $[^{212}\text{Pb}]\text{Pb-MC1L}$ but not in animals treated with 6.7 MBq at 28 weeks post-treatment. However, there was no dose-dependent change in liver injury marker concentrations with levels lower than the threshold of severe hepatocellular injury based on Hy's law (\geq three-fold rise in AST, ALT), which correlates with the low $[^{203}\text{Pb}]\text{Pb-MC1L}$ liver uptake observed (Fig. 2a).

Renal toxicity evaluation

The presentation of radiation-induced nephrotoxicity is usually late in both pre-clinical models and humans. Consistent with kidneys being frequently a treatment-limiting organ for RLTs, we observed rapid and high kidney uptake in our biodistribution and dosimetry studies (Fig. 2a), which led us to perform an in-depth kidney toxicity evaluation. In the first 8 weeks post-treatment, there was no evidence of kidney toxicity by measuring the serum endogenous kidney function biomarkers BUN and creatinine. At 28 weeks post-treatment, BUN and sCr were significantly elevated in animals treated with 3.0 and 6.7 MBq, but not 0.9 MBq $[^{212}\text{Pb}]\text{Pb-MC1L}$ compared to control mice (Fig. 5a, b). To address the low sCr sensitivity for kidney dysfunction detection in mice [19], we also measured serum cystatin C as a superior surrogate marker of kidney function at 28 weeks. Elevated cystatin C was only observed in animals injected with 6.7 MBq $[^{212}\text{Pb}]\text{Pb-MC1L}$, but not in other groups (Fig. 5c). Kidney histological analysis at 28 weeks following $[^{212}\text{Pb}]\text{Pb-MC1L}$ treatment demonstrated a significant increase in tubular injury, interstitial inflammation, glomerular changes, and fibrosis in mice treated with 6.7 MBq compared to control mice (Fig. 5d, e).

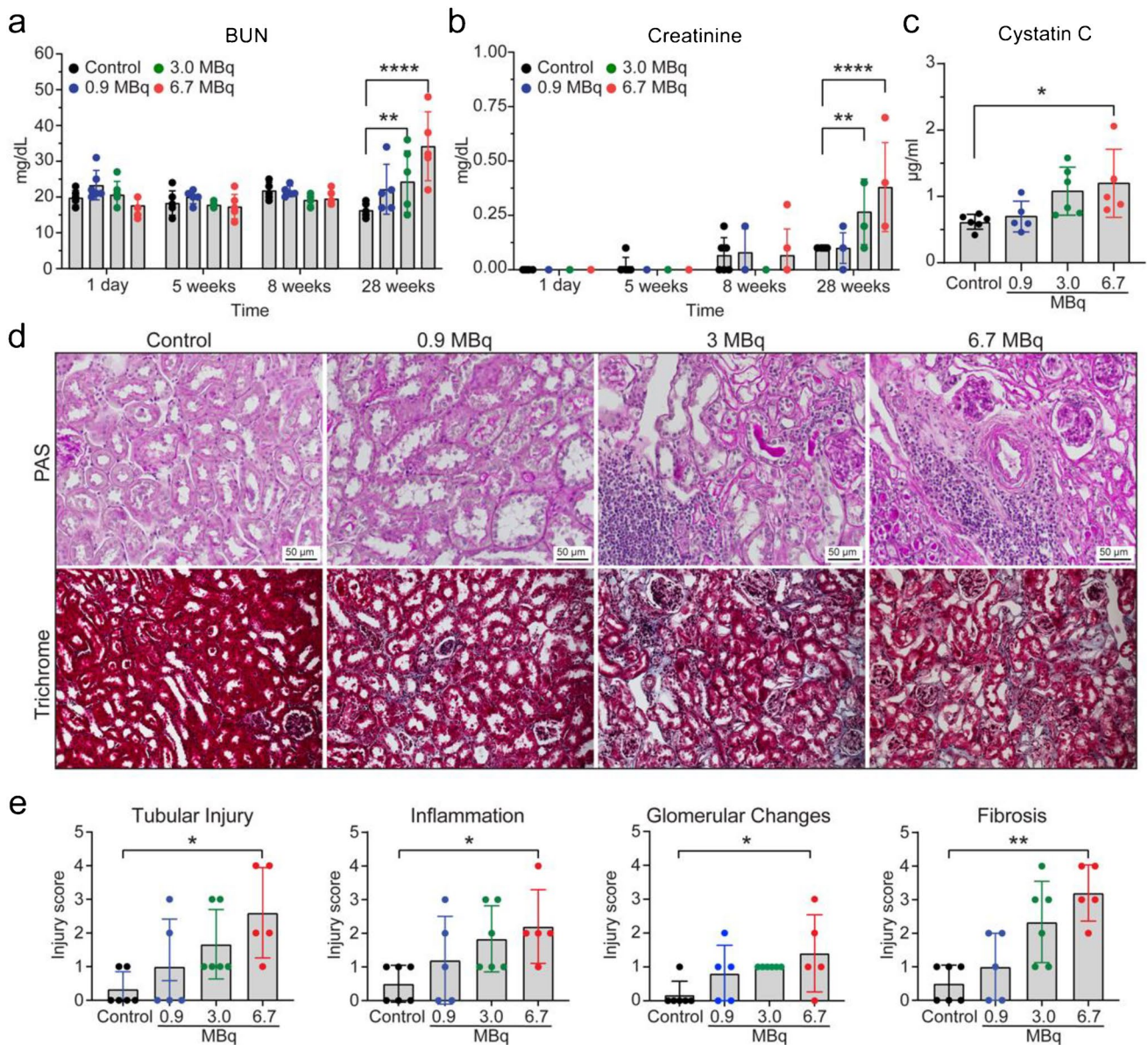


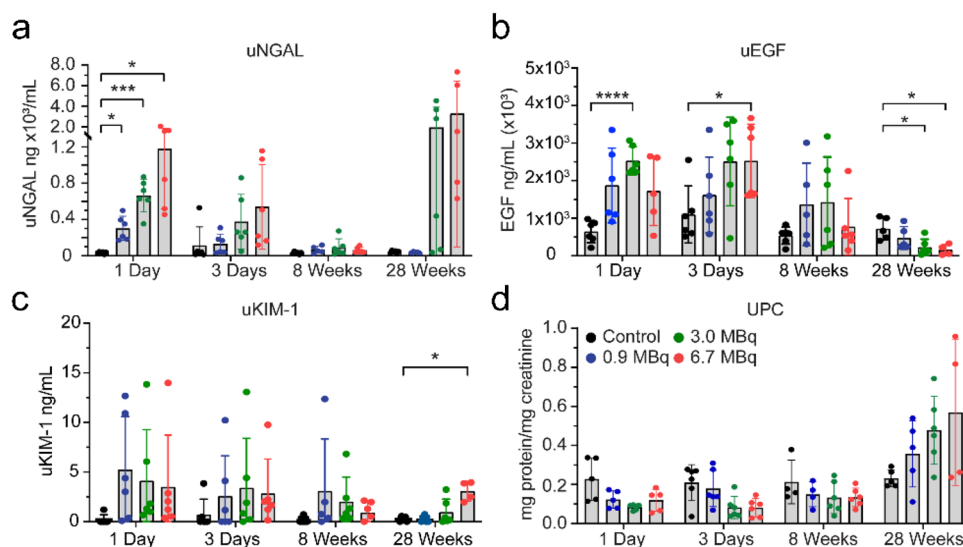
Fig. 5 **a** BUN (blood urea nitrogen), **b** serum creatinine, and **c** serum cystatin C kidney function markers. **d** Representative images of kidney sections stained by PAS (periodic acid-Schiff) and Masson’s trichrome, scale bar 50 µm. **e** Tubular injury (TI), interstitial inflammation (IF), glomerular changes (GC), and fibrosis (FIB) his-

tological scoring of kidney sections from CD-1 Elite mice at the end-of-study. Statistical analysis was made by two-way ANOVA analysis for serum biomarkers and the Kruskal–Wallis test for histological score analysis, with $*p < 0.05$

There was some evidence of tubulointerstitial injury in other treated groups that appeared to be dose-dependent; however, it was non-statistically significant (Fig. 5e). Using an injury score from 0 to 4 in all histological changes (Supplemental Table 1), the injury to the glomerular region was less severe than to the tubular and interstitial regions (Fig. 5e). Our findings highlight that kidney toxicity is more severe in the tubulointerstitium, is dose-dependent, and presents late after treatment. Moreover, we demonstrated that current diagnostic tools to evaluate nephrotoxicity are unchanged early after

treatment and present late once significant irreversible kidney damage and fibrosis occur. Using our findings and based on exponential-power regression similar to Barone et al. [20], we found that 50% normal tissue complication probability (NTCP) for our study is approximately 8.0–9.5 Gy, depending on the biological data used for modeling (fibrosis, late creatinine rise, late uNGAL rise). These results are approximately consistent with the range of expected RBE factors, and our results may inform subsequent murine experimental designs for alpha-emitting radiopharmaceuticals.

Fig. 6 Urine biomarkers. **a** NGAL (neutrophil gelatinase-associated lipocalin). **b** EGF (epidermal growth factor). **c** KIM-1 (kidney injury molecule 1). **d** UPC (urine protein:creatinine ratio). Statistical analysis was made by two-way ANOVA mixed-effect analysis with $*p < 0.05$



Urine biomarkers for AKI and correlation analysis

To test the hypothesis that RLTs cause early tubular injury that is not identified by conventional kidney function markers and that the severity of the earlier injury could correlate with long-term kidney toxicity, we measured a panel of novel biomarkers of tubular injury (NGAL and KIM-1) and tubular health (EGF) in $[^{212}\text{Pb}]\text{Pb-MC1L}$ -treated mice. We collected urine in the acute injury phase (days 1 and 3) and prospectively at 8 and 28 weeks after $[^{212}\text{Pb}]\text{Pb-MC1L}$ injection to measure urine NGAL, KIM-1, and EGF levels (Fig. 6). We also measured urine protein to creatinine ratio (UPC), a marker of hyperfiltration and a surrogate marker of glomerular damage routinely used to identify CKD progression risk [21].

There was a dose-dependent significant increase in urine NGAL (uNGAL) excretion on day 1 compared to the control group (Fig. 6a). The increase in uNGAL excretion in mice with unchanged kidney function biomarkers (BUN, sCr, Cystatin C) or proteinuria (UPC, Fig. 6d) suggests the presence of subclinical AKI caused by tubular injury. Moreover, the early increase in uNGAL positively correlated with the injected $[^{212}\text{Pb}]\text{Pb-MC1L}$ dose ($r = 0.89$, $p \leq 0.0001$), with the kidney-absorbed dose ($r = 0.89$, $p \leq 0.001$), and with the late histological alterations of TI ($r = 0.72$, $p = 0.0002$), IF ($r = 0.66$, $p = 0.001$), GC ($r = 0.58$, $p = 0.004$), and FIB ($r = 0.75$, $p \leq 0.0001$) 28 weeks post-treatment (Fig. 7, yellow rectangle, Supplemental Fig. 2). The correlation between uNGAL secretion and late kidney findings could suggest that the severity of tubular cell injury could be a driver of CKD progression.

High urinary levels of EGF (uEGF) reflect functional tubular mass and regeneration potential [22] and promote tubular cell proliferation modulating the recovery from acute kidney injury [23]. There was a significant increase in uEGF

secretion on days 1 and 3 post-treatment in mice receiving 3.0 MBq and 6.7 MBq, respectively. Conversely, there was a lower urinary secretion at 28 weeks in mice treated with 3.0 and 6.7 MBq, consistent with tubulointerstitial damage (Fig. 6b), suggesting lower tubular health [22]. The proximal tubule injury biomarker KIM-1 appeared to be elevated in acute and chronic stages. However, the concentrations were highly variable; the urinary excretion did not have an apparent dose-dependent increment in the acute phase and was only significant at 28 weeks in the group receiving the highest dose (6.7 MBq) (Fig. 6c).

UPC ratio was not statistically significant at any time point. However, it showed a dose-dependent trend toward increasing proteinuria at 28 weeks when there was already evidence of kidney dysfunction by sCr and cystatin C (Fig. 6d). Our results demonstrated that biomarkers of tubular injury and tubular health are more sensitive than endogenous biomarkers of kidney function to detect early $[^{212}\text{Pb}]\text{Pb-MC1L}$ -mediated injury.

Bone marrow toxicity

To evaluate bone marrow toxicity, we performed CBC analysis at 3 and 28 weeks following the injection of $[^{212}\text{Pb}]\text{Pb-MC1L}$ in male CD-1 Elite mice ($n = 6$) (Fig. 4a). At 3 weeks post-injection, there was no significant change in any indicative biomarker of acute bone marrow toxicity (i.e., WBC, neutrophil, lymphocyte, hemoglobin, and RBC), indicating no acute hematotoxicity resulted from $[^{212}\text{Pb}]\text{Pb-MC1L}$ treatment (Fig. 8). At the conclusion of the study (28 weeks), no significant change was observed in WBC, neutrophils, or lymphocytes in any group of mice treated with $[^{212}\text{Pb}]\text{Pb-MC1L}$ compared with the control cohort (Fig. 8a–c). However, there was an isolated reduction of hemoglobin and RBC at 28 weeks post-injection of $[^{212}\text{Pb}]\text{Pb-MC1L}$ in

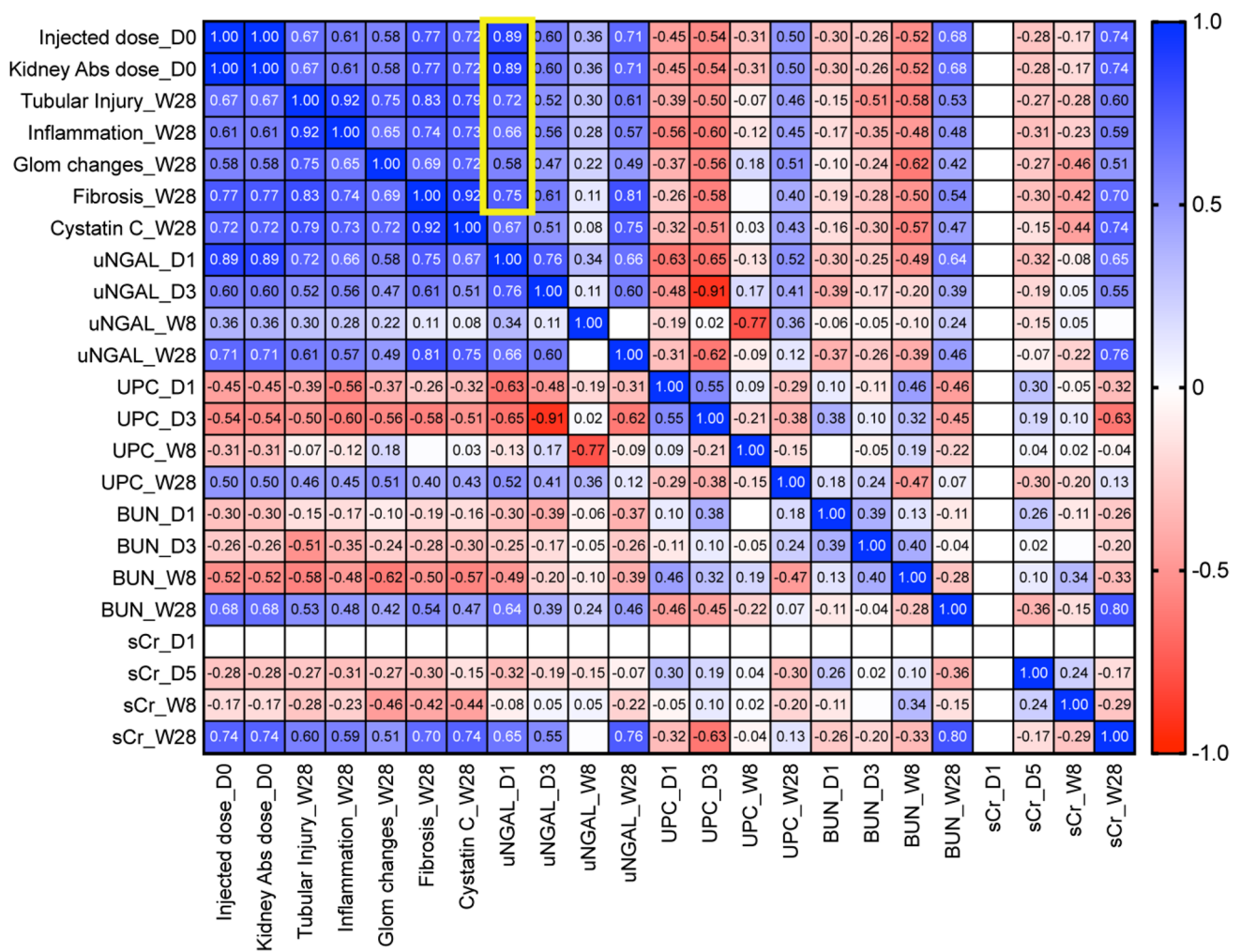


Fig. 7 Correlation analysis of injected dose, kidney damage scores, uNGAL (yellow rectangle), UPC, BUN, and sCr at each time point. Statistical analysis was made by computed nonparametric Spearman correlation for urine biomarkers and multiparameter correlation

mice treated with 3 and 6 MBq (Fig. 8d, e). Based on renal findings with evidence of CKD by histology and functional biomarkers at this stage, the isolated changes in hemoglobin and RBC could be secondary to anemia of CKD and not due to bone marrow toxicity.

Discussion

In this study, we report for the first time the use of urinary biomarkers of tubulointerstitial disease to identify subclinical AKI and predict CKD associated with α -emitter RLT in a murine model. Using $[^{203}\text{Pb}]\text{Pb-MC1L}$ to characterize the distribution and absorbed dose of $[^{212}\text{Pb}]\text{Pb-MC1L}$, kidneys appear to have the highest uptake. The dose depositions in kidneys from injection of 0.9, 3.0, and 6.7 MBq $[^{212}\text{Pb}]\text{Pb-MC1L}$ were, on average, 2.8, 8.9, and 20 Gy, respectively. The injected activities were selected to cover

low, medium, and high kidney doses intended to induce AKI. A dose-escalation toxicity study in mice was well tolerated based on body weight measurement with lack of significant hematotoxicity and liver toxicity. However, we observed the development of late CKD in mice treated with higher $[^{212}\text{Pb}]\text{Pb-MC1L}$ doses based on the profile change of kidney function biomarkers and the kidney histological alterations found 28 weeks after treatment. There was a significant dose-dependent urinary excretion of the tubular injury biomarker uNGAL the day after $[^{212}\text{Pb}]\text{Pb-MC1L}$ treatment that highly correlated with the severity of tubulointerstitial injury and late kidney function biomarkers. Despite the lack of early changes in conventional endogenous kidney function biomarkers (BUN, sCr, and serum cystatin C), the early concurrent increase in tubular injury suggests that early subclinical tubular injury could explain the long-term renal dysfunction observed at 28 weeks.

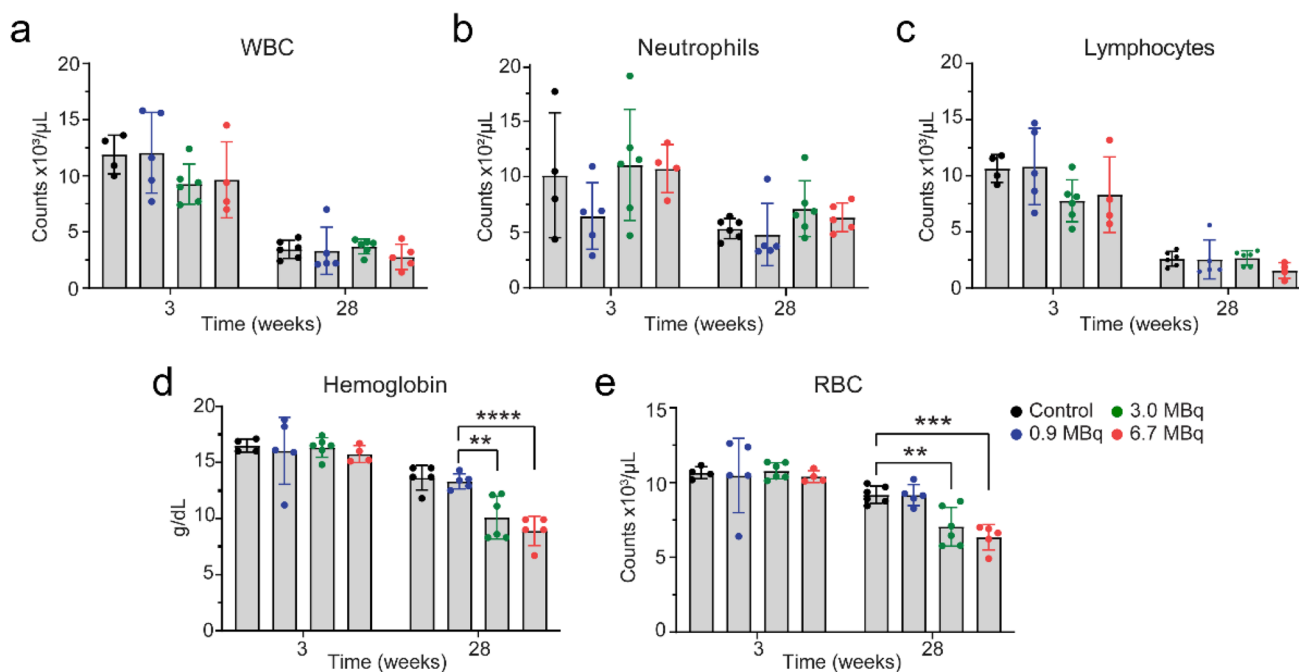


Fig. 8 Complete blood counts. **a** White blood cells (WBC). **b** Neutrophils. **c** Lymphocytes. **d** Hemoglobin. **e** Red blood cells (RBC). Statistical analysis was made by two-way ANOVA analysis with $*p < 0.05$

Dosimetry is a strategy that facilitates the determination of doses administered to normal organs, including those more sensitive to RLT toxicity. In the present study, we administered $[^{212}\text{Pb}]\text{Pb}$ -labeled peptide $[^{212}\text{Pb}]\text{Pb}$ -MC1L via *i.v.* injection to deliver α -radiation. MC1L is a synthetic peptide of 7 amino acids cyclized via Cu-mediated click chemistry. As an analog of alpha-melanocortin stimulating hormone (α -MSH), MC1L binds with melanocortin receptor 1 (MC1R) overexpressed in metastatic melanoma. Within this paradigm, the 10.6-h half-life of $[^{212}\text{Pb}]$ decay matches the relatively shorter biological half-life of small peptides compared with the long biological half-lives of antibodies [24]. Cyclotron-produced gamma-ray-emitting radionuclide $[^{203}\text{Pb}]$ was used as an elementally identical imaging surrogate for $[^{212}\text{Pb}]$ [7]. $[^{203}\text{Pb}]\text{Pb}$ -MC1L surrogate was injected in the same animal model to determine the *in vivo* biodistribution for calculating the dosimetry of $[^{203}\text{Pb}]\text{Pb}$ -MC1L in normal organs. Our prior studies have demonstrated excellent chelation kinetics and stability with PSC for $[^{212}\text{Pb}]$ and $[^{212}\text{Bi}]$ [8]. However, previous literature has shown that during a fraction of $[^{212}\text{Pb}]$ disintegrations, the daughter $[^{212}\text{Bi}]$ cations are released from the chelator [25]. Based on the known kinetics of bismuth, it is likely that some released ions will accumulate and decay in the liver and kidneys. Therefore, doses to these structures may be underestimated when utilizing $[^{203}\text{Pb}]$ as a dosimetric surrogate without accounting for these effects.

Due to its rapid clearance, we observed low $[^{203}\text{Pb}]\text{Pb}$ -MC1L liver and blood uptake and retention. We did not observe significant liver toxicity after $[^{212}\text{Pb}]\text{Pb}$ -MC1L treatment like in previous reports using $[^{177}\text{Lu}]\text{Lu}$ -DOTA-TATE [26]. Some cases of hematological toxicity (grade 3/4) and dose-dependent acute hematological toxicity have been reported in patients receiving $[^{177}\text{Lu}]\text{Lu}$ -DOTA-TATE [27] and $[^{225}\text{Ac}]\text{Ac}$ -DOTATOC [28] therapy. Hematological toxicity after RLTs increases in patients with baseline nephrotoxicity (transient or persistent elevation in sCr), probably due to the prolonged circulation time of the radiopeptide in patients with poor kidney function, which increases bone marrow exposure to radiation [29]. Our study showed a late reduction in hemoglobin and RBC 28 weeks after $[^{212}\text{Pb}]\text{Pb}$ -MC1L treatment in mice with evidence of kidney dysfunction based on BUN and sCr measurements. Because anemia is common in patients with CKD due to reduced kidney erythropoietin production, our findings suggest the late reduction in hemoglobin and RBC after $[^{212}\text{Pb}]\text{Pb}$ -MC1L treatment was secondary to anemia of CKD.

The understanding of RLT-associated nephrotoxicity in patients is limited and primarily evaluated by measuring endogenous kidney functional biomarkers, like sCr, that do not assess the severity or localization of tubulointerstitial damage. During steady-state conditions, sCr is commonly used to estimate GFR. More than half of the kidney mass must be impaired to detect an increase in sCr as a kidney

dysfunction biomarker [30], explaining the late increase in functional biomarkers after [^{212}Pb]Pb-MC1L treatment as evidence of the histological CKD progression. Moreover, sCr levels are affected by tubular secretion and reabsorption, kidney generation, extrarenal elimination, certain medications, and patient gender, age, diet, and muscle mass, which results in an overestimation of GFR and does not reflect accurately intrinsic kidney injury [31]. The reports of kidney toxicity in α -emitters are limited, and sCr restrictions may explain the controversy in nephrotoxicity development. In a study of 39 patients receiving [^{225}Ac]Ac-DOTATOC α -RLT, only 22 were suitable to evaluate long-term kidney function due to tumor progression or change in therapy. Over a median of 57 months (range 18–90 months), they observed an average eGFR-loss of 8.4 mL/min (9.9%) per year, and treatment-related kidney failure occurred in two patients after a delay of > 4 years [32]. The lack of accuracy in nephrotoxicity detection, mainly by sCr-based eGFR, led to the conclusion that kidney failure is independent of administered radioactivity and other clinical risk factors are significant or the main contributors [32–34]. Following findings in humans, we did not observe any early changes in the conventional kidney function biomarkers BUN and creatinine. We only found late significant changes at 28 weeks in mice treated with [^{212}Pb]Pb-MC1L at 3.0 and 6.7 MBq, consistent with a kidney-absorbed dose of ~8.9 and ~20 Gy, respectively. Even though no RBE scaling was used in this work to avoid ambiguity, and all doses are presented as physical absorbed dose to the structure of interest, these results are in accordance with pre-clinical studies using [^{213}Bi]Bi-DOTATATE (RBE of 4–5 for acute renal toxicity), where the calculated renal LD_{50} , at which 50% of the treated animals would develop acute nephrotoxicity, was 20 ± 8 Gy [35]. Kidney functional biomarkers (BUN and sCr) do not directly detect injury in the tubular epithelium, the leading site of injury in most forms of AKI, that, without treatment, can progress to CKD [13]. In line with radiopeptide reabsorption by proximal tubular cells, pre-clinical data in mice and rat models have shown evidence of long-term tubulointerstitial disease after β -RLTs and α -RLT in the absence of severe glomerular pathology or sCr changes [11, 12]. In this context, the delayed change in kidney function biomarkers and the lack of information on tubular injury result in poor accuracy in diagnosing acute structural kidney damage associated with RLT treatment and could result in missing valuable treatment windows to prevent CKD progression.

Biomarkers of tubular injury and health [36] are more frequently used to diagnose AKI before the loss of filtration function (kidney function biomarkers changes), supporting their potential incorporation into nephrotoxic evaluation in RLT patients. Urinary biomarkers of tubular health (EGF) and injury (KIM-1 and NGAL) measurements in mice treated with [^{212}Pb]Pb-MC1L showed an early increase in NGAL

and EGF excretion. NGAL is a protein reabsorbed by proximal tubules and released by the damaged distal tubules in response to acute tubular injury, which can be detected in the urine within hours of tubular injury [37]. Thus, an increase in urine NGAL reflects both distal tubular injury that causes an increase in NGAL production to the urine and systemic circulation and proximal tubular damage that results in a lack of NGAL reabsorption by proximal tubular cells [38]. We demonstrate that uNGAL excretion was significantly increased after [^{212}Pb]Pb-MC1L treatment with a dose-dependent pattern on day 1 after treatment. Moreover, its increased urinary excretion was highly correlated with tissue damage at 28 weeks, similar to the long-term serum NGAL increase observed in mice receiving the α -emitter [^{213}Bi]Bi-DOTATATE [35]. The early elevation in uNGAL indicates a dose-dependent [^{212}Pb]Pb-MC1L-induced tubular injury that correlates with long-term kidney toxicity. The observed early increase in tubular injury biomarkers with a lack of changes in kidney function biomarkers is used to diagnose a subclinical AKI condition [39]. This condition is usually asymptomatic and has been associated with a two- to three-fold increased risk of death or the need for kidney support therapy compared to patients with normal levels of sCr and tubular damage biomarkers [40]. EGF expression is specific for the ascending limb of Henle and distal tubules and has been associated with enhanced tubular cell regeneration and repair, accelerating kidney recovery after injury [23, 41]. uEGF is decreased in various kidney diseases in humans, including patients with CKD [42]. We found a significant initial increase in uEGF excretion in the 3 MBq and 6.7 MBq that was then significantly reduced at 28 weeks after treatment, suggesting an adequate initial response to injury with a lower late tubular reserve 28 weeks after treatment compared to the control group. Finally, KIM-1 is a protein expressed in proximal tubular epithelial cells rarely expressed in organs other than kidneys, whose increased urine level is a sensitive indicator for early proximal tubular injury, particularly for ischemic or nephrotoxic AKI patients [43]. We found a trend toward an increase in uKIM-1 after [^{212}Pb]Pb-MC1L treatment that persisted and was significant in the mice treated with 6.7 MBq after 28 weeks. The urinary biomarker patterns suggest that proximal tubule cells might not be the only tubular segment affected by [^{212}Pb]Pb-MC1L treatment.

We recognize some limitations in our study design. Studies evaluating long-term radiation-induced toxicity can be extended up to 36 weeks post-therapy [44], and our study concluded at 28 weeks (~7 months). However, the average mouse lifespan is about 24 months [45], and a follow-up of 7 months post-treatment represents approximately one-third of their lifespan. In murine CKD models, where it is expected to have a gradual renal function decline, mice are followed between 1 and 6 months post-injury to evaluate chronic changes in tissue, including

fibrosis [46]. Because mice treated with 6.7 MBq had significant changes in kidney function biomarkers suggesting clinically meaningful renal function decline, we concluded our study at 28 weeks to ensure adequate survival in each group to compare histological findings. We found significant fibrosis in that group (score 3 of 4), supporting adequate time to identify fibrosis in this model.

The results from this dose-escalation pre-clinical toxicity study propose that increased uNGAL secretion could be an additional diagnostic tool to identify patients developing α -RLT subclinical AKI and at risk of CKD. The changes in uEGF suggest that proximal tubule cells might not be the only tubular segment affected by α -RLT and highlight how potential early tubular damage could be an essential driver of long-term α -RLT-related nephrotoxicity. Together with the conventional clinical predictors of kidney health (sCr, cystatin C, UPC), urine biomarkers of tubular injury (i.e., NGAL) and tubular health (i.e., EGF) in combination with dosimetry could be used to personalize α -RLT and provide higher doses to those patients without evidence of tubulointerstitial injury. On the contrary, in patients where therapy is still required and highly beneficial, it would empower practitioners to discuss the long-term risk with patients and ensure early and close CKD follow-up to improve their outcomes, as previously proposed. More studies using dosimetry and evaluating biomarkers of tubulointerstitial disease in RLTs are needed to identify the timing of tubular injury at specific renal dosages and guide future toxicity mechanistic studies. This approach could facilitate tumor treatment maximization, development of nephroprotective therapies, and identification of patients at risk of long-term toxicity.

Supplementary Information The online version contains supplementary material available at <https://doi.org/10.1007/s00259-023-06559-9>.

Author contribution ML, CR-P: data analysis and interpretation; writing—original draft. DLiu: experiment design, sample collection, and processing. SAG: mouse and human dosimetry analysis and interpretation. GV-M, GM-A: kidney biomarkers measurement. DLee: provided consultation for Perspective Therapeutics. PR: blind PAS histological analysis. BMM: sample collection and processing. EAS: radionuclide generation. RMW: cardiotoxicity analysis. SCL: blind Masson's trichrome histological analysis. FLJ: writing—review and editing. DZ-O, MKS: conceptualization, methodology, writing—review and editing, supervision.

Funding Partial support for these studies was provided by the following grants from the US National Cancer Institute—R44CA268314, R44CA232954, R44CA250872, R44CA254613, R44CA203430, R01CA243014 (MKS), and from K12HD027748 (DZ-O).

Data availability The datasets generated during and/or analyzed during the current study are available from the corresponding author upon reasonable request.

Declarations

Ethics approval All animal studies followed the Guide for the Care and Use of Laboratory Animals and were approved by the University of Iowa Animal Care and Use Committee.

Competing interests ML, DLiu, MKS, BMM, EAS, and FLJ are employees of Perspective Therapeutics. DLee provides consultation for Perspective Therapeutics. SAG is a consultant to CDE Dosimetry Inc. and speaking honoraria from MIM Software and Voximetry. DZO has ongoing NCI funding in collaboration with Perspective Therapeutics.

Open Access This article is licensed under a Creative Commons Attribution 4.0 International License, which permits use, sharing, adaptation, distribution and reproduction in any medium or format, as long as you give appropriate credit to the original author(s) and the source, provide a link to the Creative Commons licence, and indicate if changes were made. The images or other third party material in this article are included in the article's Creative Commons licence, unless indicated otherwise in a credit line to the material. If material is not included in the article's Creative Commons licence and your intended use is not permitted by statutory regulation or exceeds the permitted use, you will need to obtain permission directly from the copyright holder. To view a copy of this licence, visit <http://creativecommons.org/licenses/by/4.0/>.

References


1. Te Beek ET, Burggraaf J, Teunissen JJM, Vriens D. Clinical pharmacology of radiotheranostics in oncology. *Clin Pharmacol Ther.* 2023;113:260–74. <https://doi.org/10.1002/cpt.2598>.
2. Miao Y, Quinn TP. Advances in receptor-targeted radiolabeled peptides for melanoma imaging and therapy. *J Nucl Med.* 2021;62:313–8. <https://doi.org/10.2967/jnumed.120.243840>.
3. Osl T, Schmidt A, Schwaiger M, Schottelius M, Wester HJ. A new class of PentixaFor- and PentixaTher-based theranostic agents with enhanced CXCR4-targeting efficiency. *Theranostics.* 2020;10:8264–80. <https://doi.org/10.7150/thno.45537>.
4. Kratochwil C, Bruchertseifer F, Giesel FL, Weis M, Verburg FA, Mottaghy F, et al. ²²⁵Ac-PSMA-617 for PSMA-targeted alpha-radiation therapy of metastatic castration-resistant prostate cancer. *J Nucl Med.* 2016;57:1941–4. <https://doi.org/10.2967/jnumed.116.178673>.
5. Navalkissoor S, Grossman A. Targeted alpha particle therapy for neuroendocrine tumours: the next generation of peptide receptor radionuclide therapy. *Neuroendocrinology.* 2019;108:256–64. <https://doi.org/10.1159/000494760>.
6. Li M, Liu D, Lee D, Cheng Y, Baumhover NJ, Marks BM, et al. Targeted alpha-particle radiotherapy and immune checkpoint inhibitors induces cooperative inhibition on tumor growth of malignant melanoma. *Cancers (Basel).* 2021;13. <https://doi.org/10.3390/cancers13153676>.
7. Li M, Sagastume EA, Lee D, McAlister D, DeGraffenreid AJ, Olewine KR, et al. (203/212)Pb theranostic radiopharmaceuticals for image-guided radionuclide therapy for cancer. *Curr Med Chem.* 2020;27:7003–31. <https://doi.org/10.2174/0929867327999200727190423>.
8. Li M, Baumhover NJ, Liu D, Cagle BS, Boschetti F, Paulin G, et al. Preclinical evaluation of a lead specific chelator (PSC) conjugated to radiopeptides for (203)Pb and (212)Pb-based theranostics. *Pharmaceutics.* 2023;15. <https://doi.org/10.3390/pharmaceutics15020414>.
9. Vejt E, de Jong M, Wetzels JF, Masereeuw R, Melis M, Oyen WJ, et al. Renal toxicity of radiolabeled peptides and antibody fragments: mechanisms, impact on radionuclide therapy, and strategies for prevention. *J Nucl Med.* 2010;51:1049–58. <https://doi.org/10.2967/jnumed.110.075101>.
10. Vejt E, Melis M, Eek A, de Visser M, Brom M, Oyen WJ, et al. Renal uptake of different radiolabelled peptides is mediated by megalin: SPECT and biodistribution studies in megalin-deficient

- mice. *Eur J Nucl Med Mol Imaging*. 2011;38:623–32. <https://doi.org/10.1007/s00259-010-1685-9>.
11. Forrer F, Rolleman E, Bijster M, Melis M, Bernard B, Krenning EP, et al. From outside to inside? Dose-dependent renal tubular damage after high-dose peptide receptor radionuclide therapy in rats measured with in vivo (99m)Tc-DMSA-SPECT and molecular imaging. *Cancer Biother Radiopharm*. 2007;22:40–9. <https://doi.org/10.1089/cbr.2006.353>.
 12. Jaggi JS, Seshan SV, McDevitt MR, LaPerle K, Sgouros G, Scheinberg DA. Renal tubulointerstitial changes after internal irradiation with alpha-particle-emitting actinium daughters. *J Am Soc Nephrol*. 2005;16:2677–89. <https://doi.org/10.1681/ASN.2004110945>.
 13. Ferenbach DA, Bonventre JV. Mechanisms of maladaptive repair after AKI leading to accelerated kidney ageing and CKD. *Nat Rev Nephrol*. 2015;11:264–76. <https://doi.org/10.1038/nrneph.2015.3>.
 14. Parihar AS, Chopra S, Prasad V. Nephrotoxicity after radionuclide therapies. *Transl Oncol*. 2022;15:101295. <https://doi.org/10.1016/j.tranon.2021.101295>.
 15. Zou C, Wang C, Lu L. Advances in the study of subclinical AKI biomarkers. *Front Physiol*. 2022;13:960059. <https://doi.org/10.3389/fphys.2022.960059>.
 16. Ix JH, Shlipak MG. The promise of tubule biomarkers in kidney disease: a review. *Am J Kidney Dis*. 2021;78:719–27. <https://doi.org/10.1053/j.ajkd.2021.03.026>.
 17. Bodei L, Cremonesi M, Ferrari M, Pacifici M, Grana CM, Bartolomei M, et al. Long-term evaluation of renal toxicity after peptide receptor radionuclide therapy with 90Y-DOTATOC and 177Lu-DOTATATE: the role of associated risk factors. *Eur J Nucl Med Mol Imaging*. 2008;35:1847–56. <https://doi.org/10.1007/s00259-008-0778-1>.
 18. Hobbs RF, Song H, Huso DL, Sundel MH, Sgouros G. A nephron-based model of the kidneys for macro-to-micro alpha-particle dosimetry. *Phys Med Biol*. 2012;57:4403–24. <https://doi.org/10.1088/0031-9155/57/13/4403>.
 19. Leelahavanichkul A, Souza AC, Street JM, Hsu V, Tsuji T, Doi K, et al. Comparison of serum creatinine and serum cystatin C as biomarkers to detect sepsis-induced acute kidney injury and to predict mortality in CD-1 mice. *Am J Physiol Renal Physiol*. 2014;307:F939–48. <https://doi.org/10.1152/ajprenal.00025.2013>.
 20. Barone R, Borson-Chazot F, Valkema R, Walrand S, Chauvin F, Gogou L, et al. Patient-specific dosimetry in predicting renal toxicity with (90)Y-DOTATOC: relevance of kidney volume and dose rate in finding a dose-effect relationship. *J Nucl Med*. 2005;46(Suppl 1):99S-106S.
 21. Qin X, Hu H, Cen J, Wang X, Wan Q, Wei Z. Association between urinary protein-to-creatinine ratio and chronic kidney disease progression: a secondary analysis of a prospective cohort study. *Front Med (Lausanne)*. 2022;9:854300. <https://doi.org/10.3389/fmed.2022.854300>.
 22. Norvik JV, Harskamp LR, Nair V, Shedden K, Solbu MD, Eriksen BO, et al. Urinary excretion of epidermal growth factor and rapid loss of kidney function. *Nephrol Dial Transplant*. 2021;36:1882–92. <https://doi.org/10.1093/ndt/gfaa208>.
 23. Humes HD, Cieslinski DA, Coimbra TM, Messana JM, Galvao C. Epidermal growth factor enhances renal tubule cell regeneration and repair and accelerates the recovery of renal function in postschemic acute renal failure. *J Clin Invest*. 1989;84:1757–61. <https://doi.org/10.1172/JCI114359>.
 24. Booth BJ, Ramakrishnan B, Narayan K, Wollacott AM, Babcock GJ, Shriver Z, et al. Extending human IgG half-life using structure-guided design. *Mabs*. 2018;10:1098–110. <https://doi.org/10.1080/19420862.2018.1490119>.
 25. Mirzadeh S, Kumar K, Gansow OA. The chemical fate of 212Bi-DOTA formed by β -decay of 212Pb(DOTA) $^{2-}$. *Radiochim Acta*. 1993;60:1–10. <https://doi.org/10.1524/ract.1993.60.1.1>.
 26. Strosberg J, El-Haddad G, Wolin E, Hendifar A, Yao J, Chasen B, et al. Phase 3 trial of (177)Lu-Dotatate for midgut neuroendocrine tumors. *N Engl J Med*. 2017;376:125–35. <https://doi.org/10.1056/NEJMoa1607427>.
 27. Bergsma H, Konijnenberg MW, Kam BL, Teunissen JJ, Kooij PP, de Herder WW, et al. Subacute haematotoxicity after PRRT with (177)Lu-DOTA-octreotate: prognostic factors, incidence and course. *Eur J Nucl Med Mol Imaging*. 2016;43:453–63. <https://doi.org/10.1007/s00259-015-3193-4>.
 28. Kesavan M, Turner JH. Myelotoxicity of peptide receptor radionuclide therapy of neuroendocrine tumors: a decade of experience. *Cancer Biother Radiopharm*. 2016;31:189–98. <https://doi.org/10.1089/cbr.2016.2035>.
 29. Svensson J, Berg G, Wangberg B, Larsson M, Forssell-Aronsson E, Bernhardt P. Renal function affects absorbed dose to the kidneys and haematological toxicity during (1)(7)(7)Lu-DOTATATE treatment. *Eur J Nucl Med Mol Imaging*. 2015;42:947–55. <https://doi.org/10.1007/s00259-015-3001-1>.
 30. Moledina DG, Parikh CR. Phenotyping of acute kidney injury: beyond serum creatinine. *Semin Nephrol*. 2018;38:3–11. <https://doi.org/10.1016/j.semnephrol.2017.09.002>.
 31. Pasala S, Carmody JB. How to use... serum creatinine, cystatin C and GFR. *Arch Dis Child Educ Pract Ed*. 2017;102:37–43. <https://doi.org/10.1136/archdischild-2016-311062>.
 32. Kratochwil C, Apostolidis L, Rathke H, Apostolidis C, Bicu F, Bruchertseifer F, et al. Dosing (225)Ac-DOTATOC in patients with somatostatin-receptor-positive solid tumors: 5-year follow-up of hematological and renal toxicity. *Eur J Nucl Med Mol Imaging*. 2021;49:54–63. <https://doi.org/10.1007/s00259-021-05474-1>.
 33. Strosberg JR, Caplin ME, Kunz PL, Ruzsiewicz PB, Bodei L, Hendifar A, et al. (177)Lu-Dotatate plus long-acting octreotide versus high-dose long-acting octreotide in patients with midgut neuroendocrine tumours (NETTER-1): final overall survival and long-term safety results from an open-label, randomised, controlled, phase 3 trial. *Lancet Oncol*. 2021;22:1752–63. [https://doi.org/10.1016/S1470-2045\(21\)00572-6](https://doi.org/10.1016/S1470-2045(21)00572-6).
 34. Bodei L, Kidd M, Paganelli G, Grana CM, Drozdov I, Cremonesi M, et al. Long-term tolerability of PRRT in 807 patients with neuroendocrine tumours: the value and limitations of clinical factors. *Eur J Nucl Med Mol Imaging*. 2015;42:5–19. <https://doi.org/10.1007/s00259-014-2893-5>.
 35. Chan HS, Konijnenberg MW, Daniels T, Nysus M, Makvandi M, de Blois E, et al. Improved safety and efficacy of (213)Bi-DOTA-TATE-targeted alpha therapy of somatostatin receptor-expressing neuroendocrine tumors in mice pre-treated with L-lysine. *EJNMMI Res*. 2016;6:83. <https://doi.org/10.1186/s13550-016-0240-5>.
 36. Jotwani VK, Lee AK, Estrella MM, Katz R, Garimella PS, Malhotra R, et al. Urinary biomarkers of tubular damage are associated with mortality but not cardiovascular risk among systolic blood pressure intervention trial participants with chronic kidney disease. *Am J Nephrol*. 2019;49:346–55. <https://doi.org/10.1159/000499531>.
 37. Lupu L, Rozenfeld KL, Zahler D, Morgan S, Merdler I, Shtark M, et al. Detection of renal injury following primary coronary intervention among ST-segment elevation myocardial infarction patients: doubling the incidence using neutrophil gelatinase-associated lipocalin as a renal biomarker. *J Clin Med*. 2021;10. <https://doi.org/10.3390/jcm10102120>.
 38. Bolignano D, Donato V, Coppolino G, Campo S, Buemi A, Lacquaniti A, et al. Neutrophil gelatinase-associated lipocalin (NGAL) as a marker of kidney damage. *Am J Kidney Dis*. 2008;52:595–605. <https://doi.org/10.1053/j.ajkd.2008.01.020>.
 39. Haase M, Kellum JA, Ronco C. Subclinical AKI—an emerging syndrome with important consequences. *Nat Rev Nephrol*. 2012;8:735–9. <https://doi.org/10.1038/nrneph.2012.197>.
 40. Haase M, Devarajan P, Haase-Fielitz A, Bellomo R, Cruz DN, Wagener G, et al. The outcome of neutrophil

- gelatinase-associated lipocalin-positive subclinical acute kidney injury: a multicenter pooled analysis of prospective studies. *J Am Coll Cardiol*. 2011;57:1752–61. <https://doi.org/10.1016/j.jacc.2010.11.051>.
41. Norman J, Tsau YK, Bacay A, Fine LG. Epidermal growth factor accelerates functional recovery from ischaemic acute tubular necrosis in the rat: role of the epidermal growth factor receptor. *Clin Sci (Lond)*. 1990;78:445–50. <https://doi.org/10.1042/cs0780445>.
 42. Tsau Y, Chen C. Urinary epidermal growth factor excretion in children with chronic renal failure. *Am J Nephrol*. 1999;19:400–4. <https://doi.org/10.1159/000013485>.
 43. Assadi F, Sharbaf FG. Urine KIM-1 as a potential biomarker of acute renal injury after circulatory collapse in children. *Pediatr Emerg Care*. 2019;35:104–7. <https://doi.org/10.1097/PEC.0000000000000886>.
 44. Stewart FA, Oussoren Y. Re-irradiation of mouse kidneys: a comparison of re-treatment tolerance after single and fractionated partial tolerance doses. *Int J Radiat Biol*. 1990;58:531–44. <https://doi.org/10.1080/09553009014551871>.
 45. Dutta S, Sengupta P. Men and mice: relating their ages. *Life Sci*. 2016;152:244–8. <https://doi.org/10.1016/j.lfs.2015.10.025>.
 46. Fu Y, Tang C, Cai J, Chen G, Zhang D, Dong Z. Rodent models of AKI-CKD transition. *Am J Physiol Renal Physiol*. 2018;315:F1098–106. <https://doi.org/10.1152/ajprenal.00199.2018>.

Publisher's Note Springer Nature remains neutral with regard to jurisdictional claims in published maps and institutional affiliations.

Authors and Affiliations

Mengshi Li¹ · Claudia Robles-Planells² · Dijie Liu¹ · Stephen A. Graves³ · Gabriela Vasquez-Martinez² · Gabriel Mayoral-Andrade² · Dongyoul Lee⁴ · Prerna Rastogi⁵ · Brenna M. Marks¹ · Edwin A. Sagastume¹ · Robert M. Weiss⁶ · Sarah C. Linn-Peirano^{2,7} · Frances L. Johnson¹ · Michael K. Schultz^{1,3,8} · Diana Zepeda-Orozco^{2,9,10} 

✉ Michael K. Schultz
mschultz@perspectivetherapeutics.com

✉ Diana Zepeda-Orozco
Diana.zepeda-orozco@nationwidechildrens.org

¹ Viewpoint Molecular Targeting, Inc. Dba Perspective Therapeutics, Coralville, IA, USA

² Kidney and Urinary Tract Center, Abigail Wexner Research Institute at Nationwide Children's, Columbus, OH, USA

³ Department of Radiology, The University of Iowa, Iowa City, IA, USA

⁴ Department of Physics and Chemistry, Korea Military Academy, Seoul, Republic of Korea

⁵ Department of Pathology, The University of Iowa, Iowa City, IA, USA

⁶ Department of Internal Medicine, The University of Iowa, Iowa City, IA, USA

⁷ Department of Veterinary Biosciences, The Ohio State University College of Veterinary Medicine Columbus, Columbus, OH, USA

⁸ Department of Radiation Oncology, Free Radical, and Radiation Biology Program, The University of Iowa, Iowa City, IA, USA

⁹ Department of Pediatrics, The Ohio State University College of Medicine, Columbus, OH, USA

¹⁰ Division of Nephrology and Hypertension, Nationwide Children's Hospital, Columbus, OH, USA